# Shrinkage mechanism and phase evolution of fine-grain BaTiO3 powder compacts containing 10 mol% BaGeO3 prepared via a precursor route

Roberto Köferstein, Lothar Jäger, Mandy Zenkner, Thomas Muller, Hans-Peter Abicht

**Materials Chemistry and Physics 112 (2008) 531–535**

**(doi:10.1016/j.matchemphys.2008.06.005)**

**http://dx.doi.org/10.1016/j.matchemphys.2008.06.005**

# Shrinkage mechanism and phase evolution of fine-grain $BaTiO_3$ powder compacts containing 10 mol% $BaGeO_3$ prepared via a precursor route

Roberto Köferstein*, Lothar Jäger, Mandy Zenkner, Thomas Müller, Hans-Peter Abicht

*Institut für Chemie/Anorganische Chemie, Martin-Luther-Universität Halle-Wittenberg, D-06099 Halle, Germany*

* Corresponding author. Tel.: +49-345-5525630; Fax: +49-345-5527028.
*E-mail address:* roberto.koeferstein@chemie.uni-halle.de

**Abstract**. The shrinkage mechanism of $BaTiO_3$ powder compacts containing 10 mol% $BaGeO_3$, synthesized by a precursor route and a conventional mixed-oxide method, are described herein. The calcination of a barium titanium germanium 1,2-ethanediolato complex precursor - $[Ba(HOC_2H_4OH)_4][Ti_{0.9}Ge_{0.1}(OC_2H_4O)_3]$ (**1**) - at 730 °C leads to a nm-sized $Ba(Ti_{0.9}/Ge_{0.1})O_3$ powder (**1a**) ($S_{BET}$ = 16.9 $m^2/g$) consisting of $BaTiO_3$ and $BaGeO_3$. Whereas the conventional mixed-oxide method yields a powder (**2**) with a specific surface area of $S_{BET}$ = 2.0 $m^2/g$. Powder compacts of **1a** start to shrink at 790 °C and the shrinkage rate reaches a maximum at 908 °C. Dense ceramic bodies can be obtained below the appearance of the liquid melt (1120 °C), therefore the shrinkage of **1a** can be described by a solid-state sintering mechanism. Otherwise the beginning of the shrinkage of powder **2** is shifted to higher temperatures and the formation of the liquid melt is necessary to obtain dense ceramic bodies.

Isothermal dilatometric investigations indicate that the initial stage of sintering is dominated by sliding processes. XRD investigations show that below a sintering temperature of 1200 °C ceramic bodies of **1a** consist of tetragonal $BaTiO_3$ and hexagonal $BaGeO_3$, whereas temperatures above 1200 °C lead to ceramics containing orthorhombic $BaGeO_3$, and a temperature of 1350 °C causes the formation of a $Ba_2TiGe_2O_8$ phase. The phase evolution of ceramic bodies of **2** is similar to **1a**, however a $Ba_2GeO_4$ phase is observed below a temperature of 1100 °C.

Keywords: ceramics; sintering; powder diffraction; heat treatment

## Introduction

$BaTiO_3$ is a basic material for a wide range of applications in the field of functional ceramics. $BaTiO_3$-based ceramics have been studied for their applications in multilayer ceramic capacitors, transducers, PTCR thermistors, etc. [1,2]. The use of additives, like $SiO_2$, $Pb_5Ge_3O_{11}$ or $B_2O_3$, enables to fabricate dense $BaTiO_3$ ceramics at low temperatures [3,4,5]. In many cases, the better densification at low sintering temperatures is achieved by the formation of a liquid phase [5,6,7,8,9]. *Völtzke* and *Abicht* [3] investigated the influence of different additives on the densification behaviour of $BaTiO_3$. They could show that the major part of densification takes place before a liquid phase is formed. In a previous paper [10] we made similar observations using $BaGeO_3$ as a sintering additive. Up to now, the influence of $BaGeO_3$ on the sintering behaviour of $BaTiO_3$ has rarely been investigated. *Guha* and *Kolar* [11] described the $BaGeO_3$-$BaTiO_3$ system as a simple binary-eutectic system with a eutectic composition of 68 mol% $BaGeO_3$ and a melting temperature of 1120 ± 5 °C.

This publication reports on the shrinkage mechanism of powder compacts of nm-sized $BaTiO_3$ powder containing 10 mol% $BaGeO_3$ prepared by decomposition of an 1,2-ethanediolato complex precursor in comparison with a powder obtained by a conventional

mixed-oxide method. In addition, comparative XRD investigations of ceramic bodies prepared by both methods have been made.

## 2. Experimental

### *2.1. Material preparation*

The preparation procedure of $[Ba(HOC_2H_4OH)_4][Ti_{0.9}Ge_{0.1}(OC_2H_4O)_3]$ (**1**) and the resulting nm-sized $Ba(Ti_{0.9}/Ge_{0.1})O_3$ (**1a**) powder has been described in detail in a previous paper [10]. Powder **1a** has a Ba/Ti ratio of 1.117 (calc. 1.111) and a Ba/(Ti+Ge) ratio of 0.999 (calc. 1.000)). The powder was milled with $ZrO_2$-balls in propan-2-ol for 2 h ($m_{powder}$:$m_{balls}$ = 1:4). After filtering and drying the powder was mixed with 5 mass% of a saturated aqueous solution of polyvinyl alcohol as a pressing aid, then the powder was pressed to discs with a green density of 2.7–2.8 g/cm$^3$. For comparison, $Ba(Ti_{0.9}/Ge_{0.1})O_3$ powder (**2**) was also prepared by a conventional mixed-oxide method. $BaCO_3$ (Sabed VL 600, *Solvay*, Germany), $TiO_2$ (Merck 808, *Merck*, Germany) and $GeO_2$ (*Acros Organics*, Belgium) were milled with a molar ratio of 10:9:1 for 24 h using $ZrO_2$-balls in propan-2-ol ($m_{powder}$:$m_{balls}$:$m_{propan\text{-}2\text{-}ol}$ = 1:1:4). After filtering off and drying the mixture was calcined in a Pt-crucible in static air at 1100 °C for 2 h (10 K/min). The remaining steps are identical to those mentioned above (as for **1a**). Analytical investigations [10] of powder **2** indicated a Ba/Ti ratio of 1.115 and a Ba/(Ti+Ge) ratio of 0.997.

### *2.2. Analytical methods*

X-ray powder diffraction (XRD) patterns were recorded by a STADI MP diffractometer from *STOE* (Germany) at 25 °C using $CoK\alpha_1$ radiation and a resolution of 0.02° for $2\theta$. The shrinkage behaviour was studied in situ by dilatometry. The dilatometric investigations were performed in a TMA 92-16.18 unit from *Setaram* (France), and the densities of these discs were calculated assuming an isotropic shrinkage behaviour. The specific surface area was

measured by the BET method using $N_2$ as an adsorption gas (Nova 1000, *Quantachrome Corporation*, USA).

## 3. Results and discussion

Recently, we have reported on the preparation procedure of a nm-sized $Ba(Ti_{0.9}/Ge_{0.1})O_3$ powder (**1a**) and the resulting ceramic bodies. [10]. Briefly, $[Ba(HOC_2H_4OH)_4][Ti_{0.9}Ge_{0.1}(OC_2H_4O)_3]$ (**1**) was calcined by the following thermal treatment: heating to 550 °C with a heating rate of 10 K/min, then slow heating with 1 K/min to 730 °C, dwelling time 30 min and followed by cooling at 10 K/min. The resulting powder (**1a**) has a specific surface area of $S_{BET}$ = 16.9 $m^2/g$ ($d_{av.}$ = 61 nm) and consists of a mixture of $BaTiO_3$ and $BaGeO_3$ (denoted as: $Ba(Ti_{0.9}/Ge_{0.1})O_3$). As found elsewhere [11] the maximum solid solubility of $BaGeO_3$ in $BaTiO_3$ was detected to be 1.8 mol%. A conventional $Ba(Ti_{0.9}/Ge_{0.1})O_3$ powder (**2**), obtained by a classical mixed-oxide process (1100 °C, 2 h), has a specific surface area of 2.0 $m^2/g$ ($d_{av.}$ = 508 nm). Fig. 1 shows SEM images of powder **1a** and **2**.

Fig. 2 shows the shrinkage behaviour (non-isothermal, 10 K/min) of powder compacts of **1a** and **2**. The shrinkage of **1a** starts at 790 °C and the shrinkage rate reaches a maximum of -1.8 %/min at 908 °C. 70 % of the whole non-isothermal shrinkage process are done up to 1000 °C. A second weak and broad maximum is observed at about 1047 °C (-0.5 %/min). The shrinkage process is nearly completed and the density rises to 91 % of the theoretical value (5.85 $g/cm^3$ [10,12]) before the eutectic temperature between $BaTiO_3$ and $BaGeO_3$ of 1120 °C is reached [11]. Therefore the shrinkage behaviour of **1a** can be described as a solid state sintering process. Powder compacts of **2** slowly start to shrink at 894 °C, but a clear and fast shrinkage process begins considerably above 950 °C. The first maximum of the shrinkage rate of -1.5 %/min is observed at 1058 °C. A shoulder at 1119 °C (-1.1 %/min) indicates the appearance of a second maximum of the shrinkage rate, which correlates with the formation

of the eutectic liquid phase. In contrast to **1a**, up to 1120 °C the compacts of **2** reach a relative density of only 67 %. Consequently, the temperature range of liquid phase sintering (≥ 1120 °C) is required for a sufficient shrinkage.

The observed shrinkage rates at the first maxima of **1a** and **2** are very high ($d(\Delta L/L_0)/dt$ = -1.5 – -1.8 %/min) and cannot only be explained by diffusion processes. Diffusion as the dominant process causes only shrinkage rates of about $10^{-4}$–$10^{-1}$ %/min [13]. Therefore the observed shrinkage rates hint that the shrinkage is mainly caused by sliding processes of whole grains. In particular for metallic systems, these processes are also described as superplastic deformation [13,14].

Isothermal dilatometric investigations allow to determine the dominant shrinkage mechanism and to calculate the activation energy. The samples for these investigations were heated with a rate of 20 K/min. The heating rate was lowered to 10 K/min 50 K before the isothermal ramp was reached. The investigations for compacts of **1a** were carried out at several isothermal ramps between 810–930 °C. The temperature range for powder **2** was set between 950–1080 °C, because we did not observe a sufficient shrinkage below 950 °C. Fig. 3 demonstrates the general approach of the isothermal dilatometric investigations [3]. The isothermal part (150 min) was separated from the shrinkage curve and the initial values were set to zero. A representation of the logarithm of $\Delta L/L_0$ versus the logarithm of time ($t$) allows to verify the dominating shrinkage mechanism [3,15]. As exemplarily shown in Fig. 3b, the isothermal shrinkage process is divided into two sections (different slopes). According to the general shrinkage equation (I) these different slopes represent different shrinkage mechanisms [15]:

$$\left(\frac{\Delta L}{L_0}\right)^{m/2} = -\frac{H}{2^m R^n} t \qquad \text{(I)}$$

Here, $\Delta L/L_0$ is the relative shrinkage, $H$ is a function containing material parameters, $R$ is the radius of the particles, $t$ is the time, $n$ and $m$ are numerical exponents depending on the

shrinkage mechanism ($m$ = 2 → viscous flow; $m$ = 5 → lattice diffusion from the grain boundary; $m$ = 6 → grain boundary diffusion).

The first segment represents the major part of the total isothermal shrinkage. The slope reveals a shrinkage exponent ($m$) of about 2, which indicates viscous flow as the dominant shrinkage mechanism. The slope of the second segment is equal to a shrinkage exponent of $m$ = 5–6 in equation I. From this it follows that grain boundary diffusion and volume diffusion from the grain boundaries are the dominating mechanisms in the second isothermal segment. The sintering mechanisms do not change with the temperature, however, the time period of each segment depends on the temperature, e.g. at a isothermal ramp of 810 °C (powder **1a**), the first segment (viscous flow) requires about the first 110 min and at 820 °C the first 60 min. Whereas temperatures of 870 and 900 °C reveals that viscous flow is the dominant mechanism only in the first 9 and 3 min, respectively. Compacts of powder **2** show the same tendency, viscous flow dominates the first 45 min at 950 °C and at 1050 °C the first 3 min. It can be noticed that the major part of the sintering process is determined by sliding and diffusion processes.

*Anderson* [16] calculated an activation energy (isothermal dilatometry) of 469 kJ/mol for the initial stage of sintering of pure $BaTiO_3$ compacts, whereas *Chen* et al. [17] obtained an activation energy of 1098 kJ/mol. It has been demonstrated by *Lin* et al. [18] that the activation energy depends on the Ba/Ti ratio. The densification of pure $BaTiO_3$ is described as a grain boundary diffusion mechanism [16,17,19]. However, *Völtzke* and *Abicht* [20] investigated some $BaTiO_3$ powders with various median grain sizes between 1.5 – 13.5 µm and they could detect viscous flow as the dominating mechanism in the early stage of sintering. The same observations were made by *Dror* et al. [21] using a $BaTiO_3$ powder with an average crystallite size of 50 nm.

On the basis of the first segment of the isothermal dilatometric investigations, we determined the activation energy for sintering using the common *Arrhenius* approach [22,23]. For

compacts of powder **1a** an activation energy of 313 ± 15 kJ/mol was calculated, while for powder **2** an activation energy of 407 ± 39 kJ/mol was obtained. It can be seen that the activation energy for the nm-sized $Ba(Ti_{0.9}/Ge_{0.1})O_3$ powder (precursor route) is considerably lower than for the coarse grained powder (mixed-oxide method). These results suggest that the reduction of the activation energy from powder **2** to **1a** is caused by smaller particle sizes. Investigations by *Dror* et al. [21] have shown that the sliding processes (rearrangement) correlate with the high amount of grain boundaries in nano $BaTiO_3$ powders. They regarded the grain boundaries as amorphous areas surrounding crystalline cores, which promotes the sliding processes. Another reason for the lower activation energy is the more homogeneous distribution of the additive in powder **1a** [3]. The lower activation energies and thus the better sintering behaviour of $Ba(Ti_{0.9}/Ge_{0.1})O_3$) powder compacts, compared with pure coarse and fine grained $BaTiO_3$ (see also ref. [10]), can be explained by sliding processes of whole grains, which are supported by the additive. *Geguzin* [13,24] explained these sliding processes with the existence of amorphous contact boundaries. Using $SiO_2$ as an additive, the formation of a glass-like Ba-Ti-Si-O intermediate was found [3,25]. Glass-like phases as a precondition for such sliding processes were also described for other systems [26,27]. Possibly, analogous amorphous Ba-Ti-Ge-O phases, during the sintering of $Ba(Ti_{0.9}/Ge_{0.1})O_3$ powder compacts, could have been formed, however, further investigations are necessary. XRD investigations (see below) reveal that the preceramic powder **1a** consists of $BaTiO_3$ as the only crystalline phase, whereas the $BaGeO_3$ phase is X-ray amorphous. At higher temperatures we observe the formation of a crystalline Ba-Ti-Ge-O phase in both samples (**1a** and **2**).

The final bulk densities of ceramic bodies (calculated from their weight and geometric dimensions) of **1a** and **2** after an isothermal sintering procedure in a muffle furnace (1 h, rate: 10 K/min) are represented in Fig. 4. Using powder compacts of **1a** we obtain dense ceramic bodies (relative density > 90 %) considerably below the eutectic temperature [10]. A sintering temperature of 1000 and 1100 °C leads to ceramics with a relative density of 94 and 95 %,

respectively. Temperatures above the eutectic temperatures cause only a marginal increase of the bulk density (1150 °C → 97 %). On these conditions, ceramic bodies of **2** have a relative density of only 62 and 88 % after sintering at 1000 and 1100 °C, respectively. Dense ceramics with more than 90 % of the theoretical density will be obtained only by liquid phase sintering (>1100 °C).

Fig. 5 and 6 show the X-ray powder patterns of these ceramics bodies as well as the preceramic powders **1a** and **2**. The XRD pattern of the preceramic powder **1a** shows only reflexions of a (pseudo)-cubic $BaTiO_3$ phase and traces of $BaCO_3$ [28]. As shown elsewhere [10] reflexions of a crystalline $BaGeO_3$ phase appears only at a calcination temperature above 800 °C. Up to a sintering temperature of 1200 °C the resulting ceramic bodies consist of tetragonal $BaTiO_3$ and hexagonal $BaGeO_3$ [28]. Sintering at 1250 °C leads to an appearance of an orthorhombic $BaGeO_3$ phase [28] and to a disappearance of hexagonal $BaGeO_3$. Higher sintering temperatures cause the formation of a crystalline $Ba_2TiGe_2O_8$ phase [28,29].

The crystalline phases of ceramics prepared via the mixed-oxide method differ slightly from the precursor method. The preceramic powder **2** reveals reflexions of tetragonal $BaTiO_3$ and orthorhombic $Ba_2GeO_4$ [28], because the conventional reaction between $BaCO_3$ and $GeO_2$ leads at first to the formation of $Ba_2GeO_4$ [30]. A ceramic body, sintered at 1000 °C, shows the same diffraction pattern as preceramic powder **2**. Only a sintering temperature of 1100 °C causes the appearance of a hexagonal $BaGeO_3$ phase. Above a sintering temperature of 1200 °C the ceramic bodies consist of tetragonal $BaTiO_3$ and orthorhombic $BaGeO_3$. Traces of a crystalline $Ba_2TiGe_2O_8$ phase appear only after a heating time of 2 h at 1350 °C. After 5 h dwell time orthorhombic $BaGeO_3$ completely disappeared and $Ba_2TiGe_2O_8$ is the only crystalline phase besides $BaTiO_3$.

## Conclusions

The shrinkage behaviour and the crystalline composition of $BaTiO_3$ ceramic bodies, containing 10 mol% $BaGeO_3$, prepared by a complex precursor method (**1a**) and a conventional mixed-oxide method (**2**) were investigated. Non-isothermal dilatometric and isothermal sintering investigations of powder compacts of **1a** (particle size: $d_{av.}$ = 61 nm) reveal that the shrinkage/densification process can be described as a solid state sintering process. The compacts start to shrink at 790 °C and the shrinkage is nearly completed below 1120 °C (eutectic temperature). By contrast, the gradual beginning of the shrinkage of powder compacts of **2** (particle size: $d_{av.}$ = 508 nm) is shifted to 894 °C and a sufficient shrinkage, and thus dense ceramic bodies, can be obtained only by liquid phase sintering above 1120 °C. Isothermal shrinkage studies show that in both cases the shrinkage of the powder compacts is characterized by sliding and diffusions processes. The activation energy for the initial stage of sintering of powder **1** was calculated to 313 ± 15 kJ/mol, whereas powder **2** has a higher activation energy of 407 ± 39 kJ/mol. After isothermal sintering up to 1200 °C for 1 h ceramic bodies of **1a** consist of tetragonal $BaTiO_3$, as the major phase, and hexagonal $BaGeO_3$. Sintering above 1200 °C leads to an orthorhombic $BaGeO_3$ phase and at 1350 °C to a $Ba_2TiGe_2O_8$ phase. Ceramics of **2** reveal only reflexion of $Ba_2GeO_4$ besides tetragonal $BaTiO_3$ at a sintering temperature of 1000 °C. Hexagonal $BaGeO_3$ appears between 1100–1200 °C, and higher temperatures leads to the formation of orthorhombic $BaGeO_3$. In contrast to **1a** the $Ba_2TiGe_2O_8$ phase is only obtained after a prolonged sintering time at 1350 °C.

***Acknowledgements***

Financial support by the Federal State Saxony-Anhalt (Cluster of Excellence "Nanostructured Materials") is gratefully acknowledged.

**References**


[1] B. Huybrechts, K. Ishizaki, M. Takata, *J. Mater. Sci.* 30 (1995) 2463-2474

[2] S.-F. Wang, G. O. Dayton, *J. Am. Ceram. Soc.* 82 (1999) 2677-2682

[3] D. Völtzke, H.-P. Abicht, *Solid State Sci.* 2 (2000) 149-159

[4] S. O. Yoon, J. H. Lung, H. Ki, *Yoop Hakhoechi* 28(5) (1991) 359-364

[5] H.-P. Jeon, S.-K. Lee, S.-W. Kim, D.-K. Choi, *Mater. Chem. Phys.* 94 (2005) 185-189

[6] J.-C. M'Peko, J. Portelles, G. Rodriguez, *J. Mater. Sci. Lett.* 16 (1997) 1850-1852

[7] G. Liu, R. D. Rosemann, *J. Mater. Sci.* 34 (1999) 4439-4445

[8] D. Kolar, D. Suvorov, *Vestn. Slov. Kem. Drus.* 28(4) (1981) 357-66

[9] S.-F. Wang, W. Huebner, J. P. Dougherty in: R. K. Pandey, M. Liu, A. Safari (Ed.), *ISAF '94, Proceedings of the 9th IEEE International Symposium on Applications of Ferroelectrics* (University Park, Pennsylvania, USA) 1994, Institute of Electrical and Electronics Engineers, New York, 1994, pp. 581-584.

[10] R. Köferstein, L. Jäger, M. Zenkner, H.-P. Abicht, *J. Mater. Sci.* 43 (2008) 832-838

[11] J. P. Guha, D. Kolar, *J. Mater. Sci.* 7 (1972) 1192-1196

[12] G. W. Marks, L. A. Monson, *Ind. Eng. Chem.* 47(8) (1955) 1611-1620

[13] W. Schatt, Sintervorgänge, VDI-Verlag, Düsseldorf 1992, pp.78-100

[14] I. I. Novikov, V. K. Portnoj, Superplastizität von Legierungen, Deutscher Verlag für Grundstoffindustrie, Leipzig, 1984, p.12 et seqq.

[15] M. N. Rahaman, Ceramic Proceeding and Sintering, Marcel Dekker, New York, 1995, pp. 398 et seqq.

[16] H. U. Anderson, *J. Am. Ceram. Soc.* 48(3) (1965) 118-121

[17] Z. C. Chen, T. A. Ring, *Ceram. Trans.* 32 (1993) 275-284

[18] M.-H. Lin, J.-F. Chou, H.-Y. Lu, *J. Eur. Ceram. Soc.* 20 (2000) 517-526

[19] L. A. Xue, Y. Chen, E. Gilbart, R. J. Brook, *J. Mater. Sci.* 25 (1990) 1423-1428

[20] D. Völtzke, H.-P. Abicht, *J. Mater. Sci. Lett.* 19 (2000) 1951-1953

[21] Y. Dror, R. D. Levi, S. Baltianski, Y. Tsur, *J. Electrochem. Soc.* 153(7) (2006) F137-F143

[22] J. J. Bacmann, G. Cizeron, *J. Am. Ceram. Soc.* 51(4) (1968) 209-212

[23] H.-P. Abicht, D. Völtzke, H. Schmidt, *Mater. Chem. Phys.* 51 (1997) 35-41

[24] Ya. E. Geguzin, Yu. I. Klinchuk, *Poroshkovaya Metallurgiya* 7 (1976) 17-25

[25] S. Senz, A. Graff, D. Hesse, H.-P. Abicht, *J. Eur. Ceram. Soc.* 20 (2000) 2469-2475

[26] G. Pezzotti, K. Ota, H.-J. Kleebe, *J. Am. Ceram. Soc.* 80 (1997) 2341-2348

[27] H.D. Ackler, Y.M. Chiang, *J. Am. Ceram. Soc.* 80 (1997) 1893-1896

[28] PDF 2 (International Centre for Diffraction Data, Pennsylvania) $BaCO_3$ [5-378], $BaTiO_3$ [72-138$_{tetragonal}$; 31-174$_{cubic}$], $BaGeO_3$ [30-127$_{hexagonal}$; 37-137$_{orthorhombic}$], $Ba_2GeO_4$ [39-1257], $Ba_2TiGe_2O_8$ [44-560]

[29] T. Höche, S. Esmaeilzadeh, R. Uecker, S. Lidin, W. Neumann, *Acta Cryst.* B59 (2003) 209-216

[30] P. Royen, G. Wilhelmi, A. Kreher, *Naturwissenschaften* (1965) 390

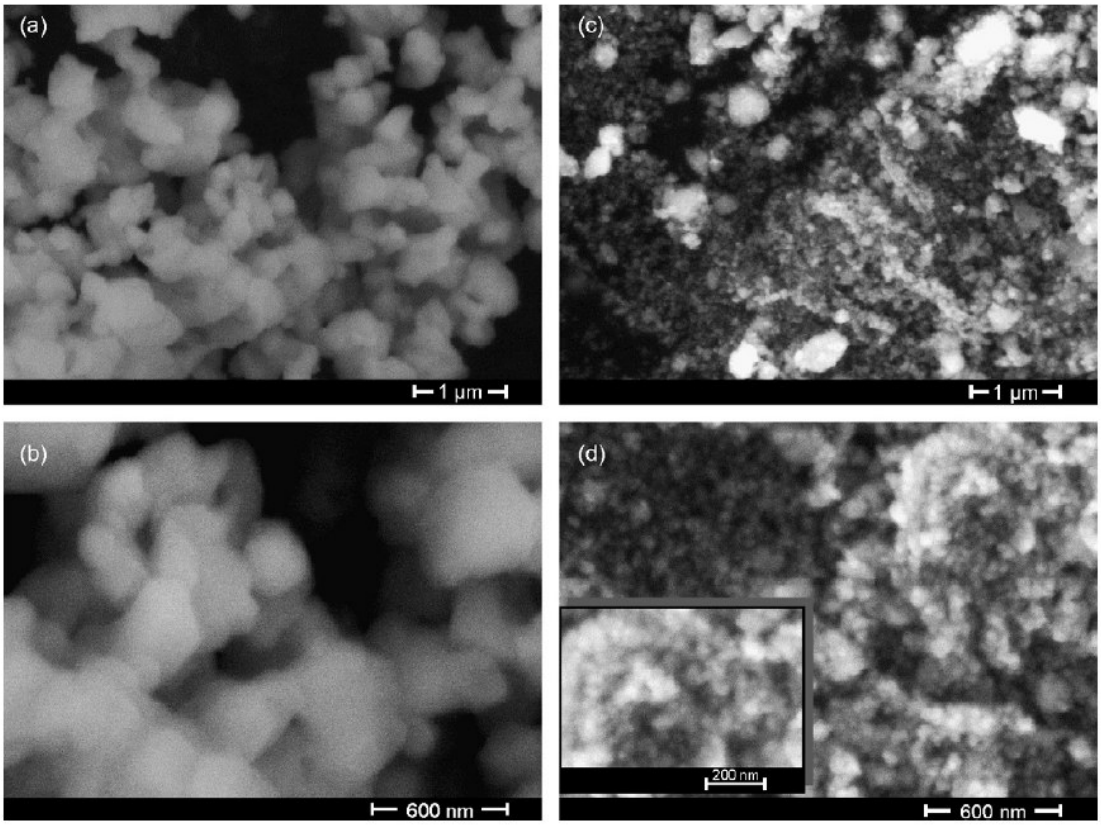


**Fig. 1.** SEM images of powder **2** (a, b) and **1a** (c, d).

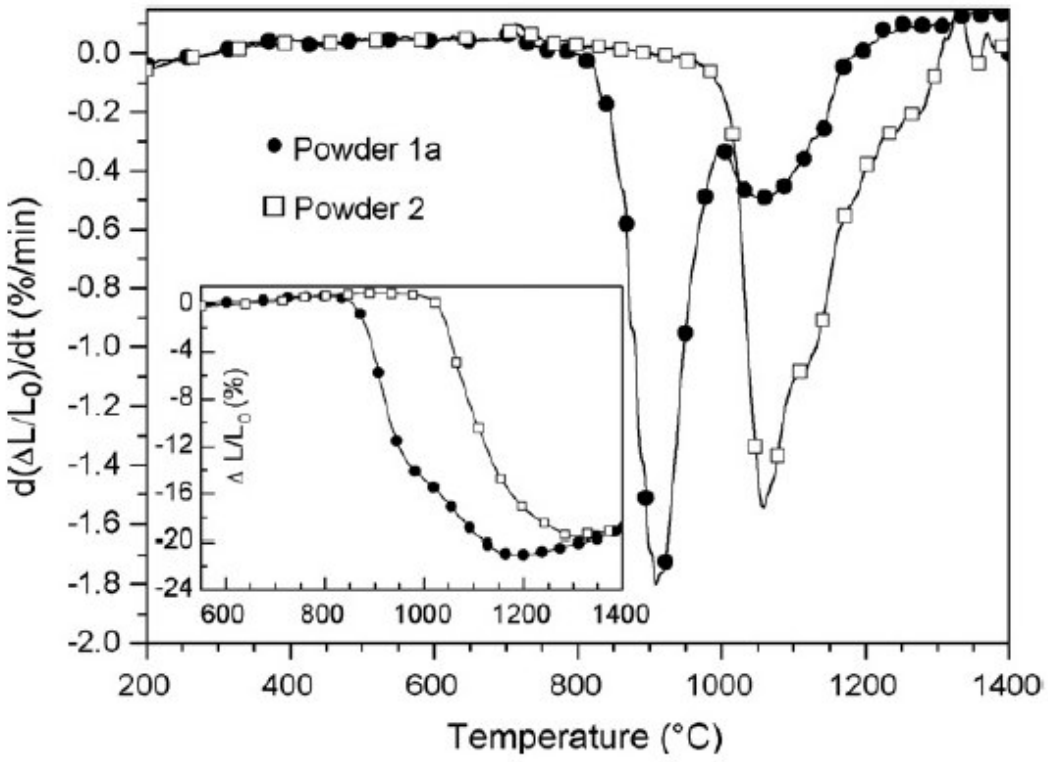


**Fig. 2.** Shrinkage rates (non-isothermal, heating rate 10 K $min^{-1}$) of green bodies of **1a** and **2**, respectively. The inset shows the relative shrinkage ($\Delta L/L_0$) of these bodies (green density: 2.7 g $cm^{-3}$).

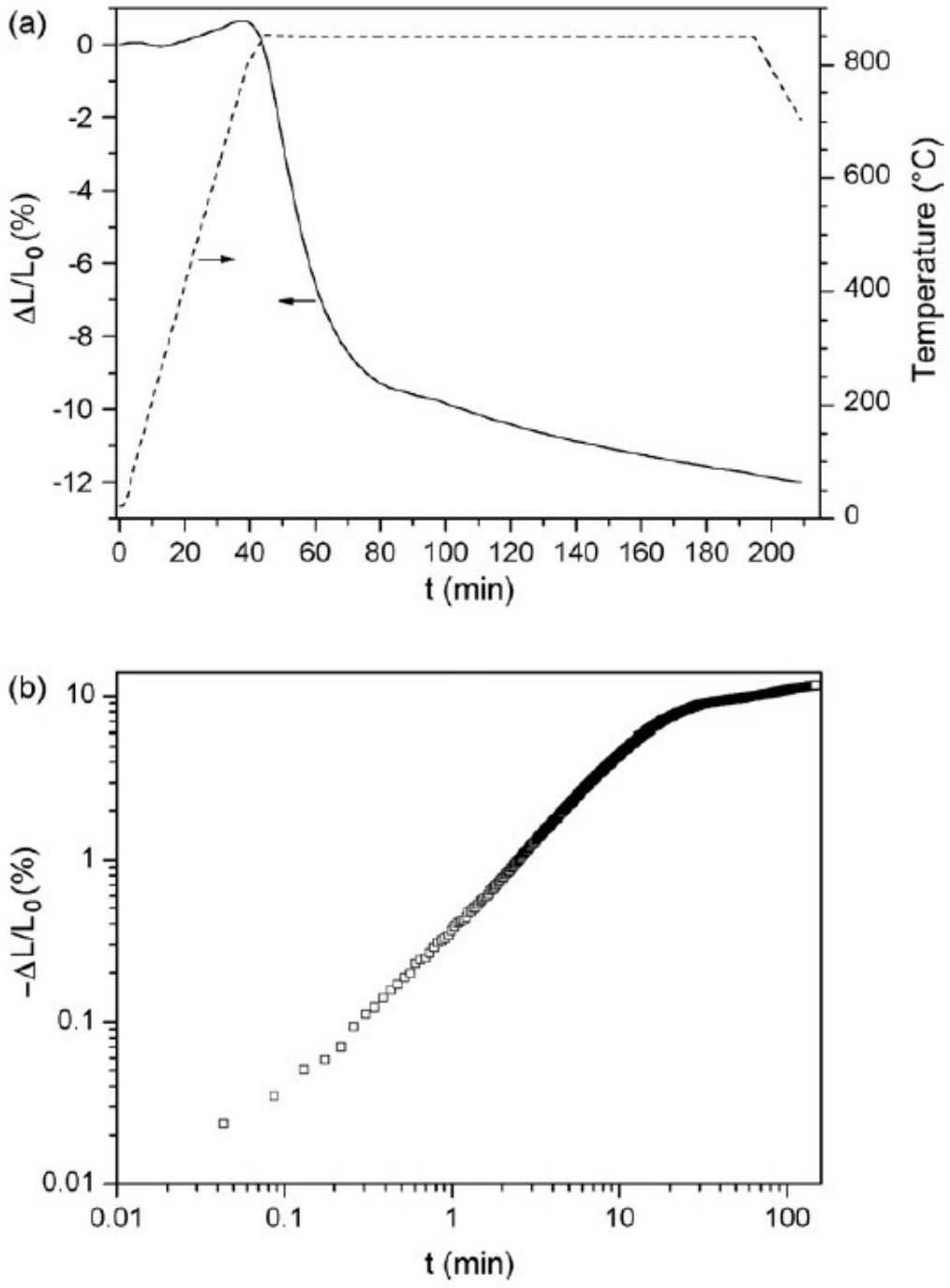


**Fig. 3.** General procedure of the isothermal dilatometric investigations demonstrated for powder **1a** at 850 °C, (a) plot of the shrinkage curve, (b) double logarithmic plot of the isothermal segment (the initial value of $\Delta L/L_0$ was set to $\Delta L/L_0 = 0$).

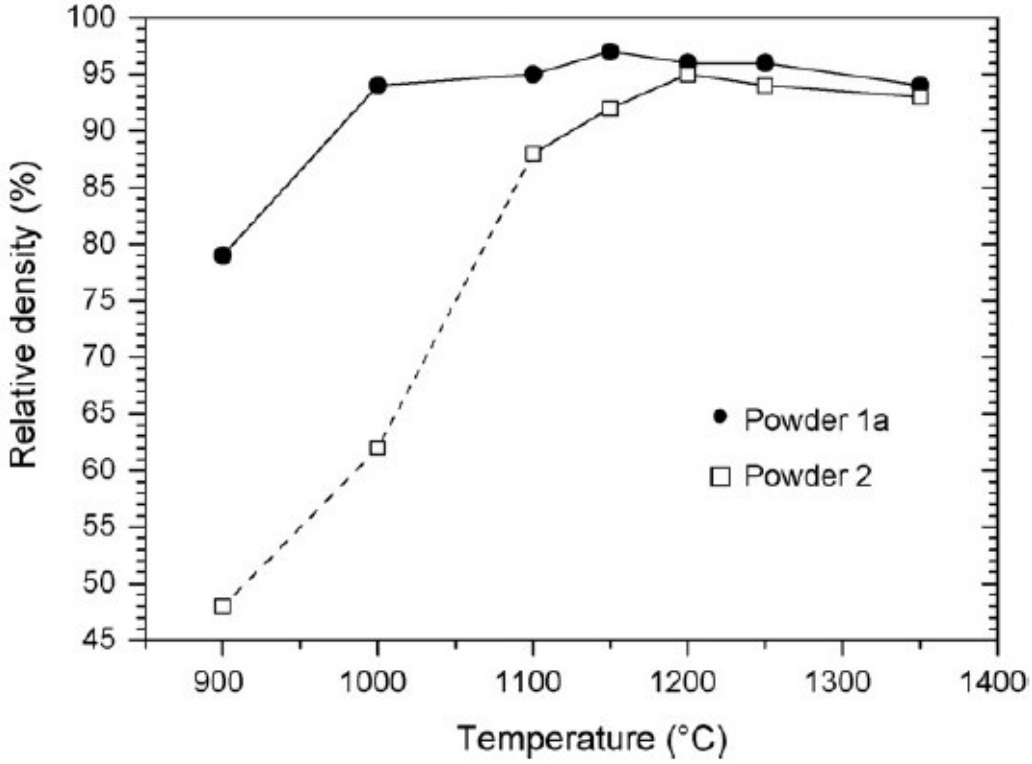


**Fig. 4.** Final densities of ceramic bodies of **1a** and **2** after an isothermal sintering process (1 h) at different temperatures in a muffle furnace. The relative densities are consistently related to the theoretical density of 5.85 g $cm^{-3}$.

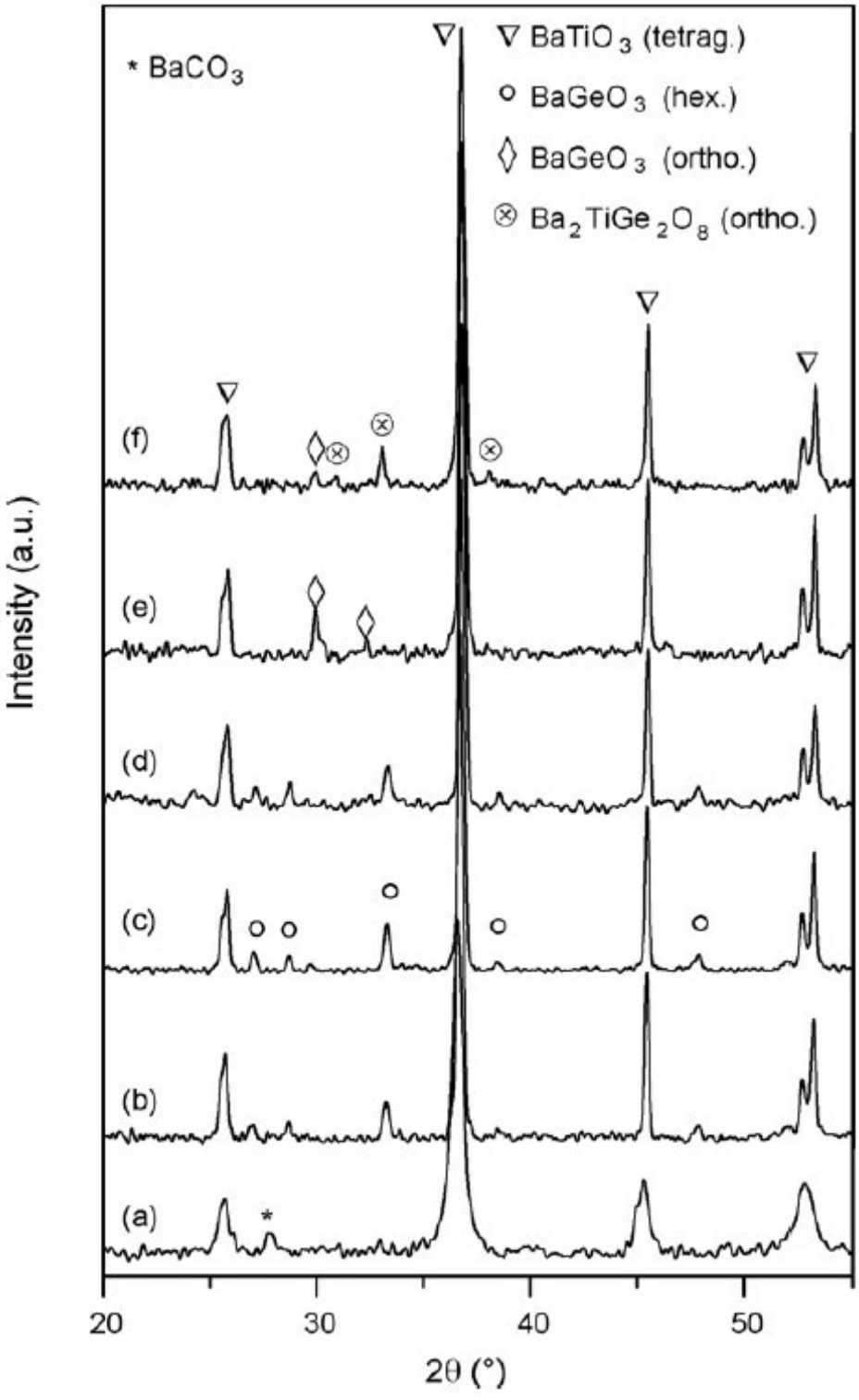


**Fig. 5.** X-ray powder diffraction patterns (recorded at 25 °C) of powder **1a** (a) and the resulting ceramic bodies after isothermal sintering (heating rate 10 K min$^{-1}$, dwelling time 1 h), (b) 1000 °C, (c) 1100 °C, (d) 1150 °C, (e) 1250 °C and (f) 1350 °C.

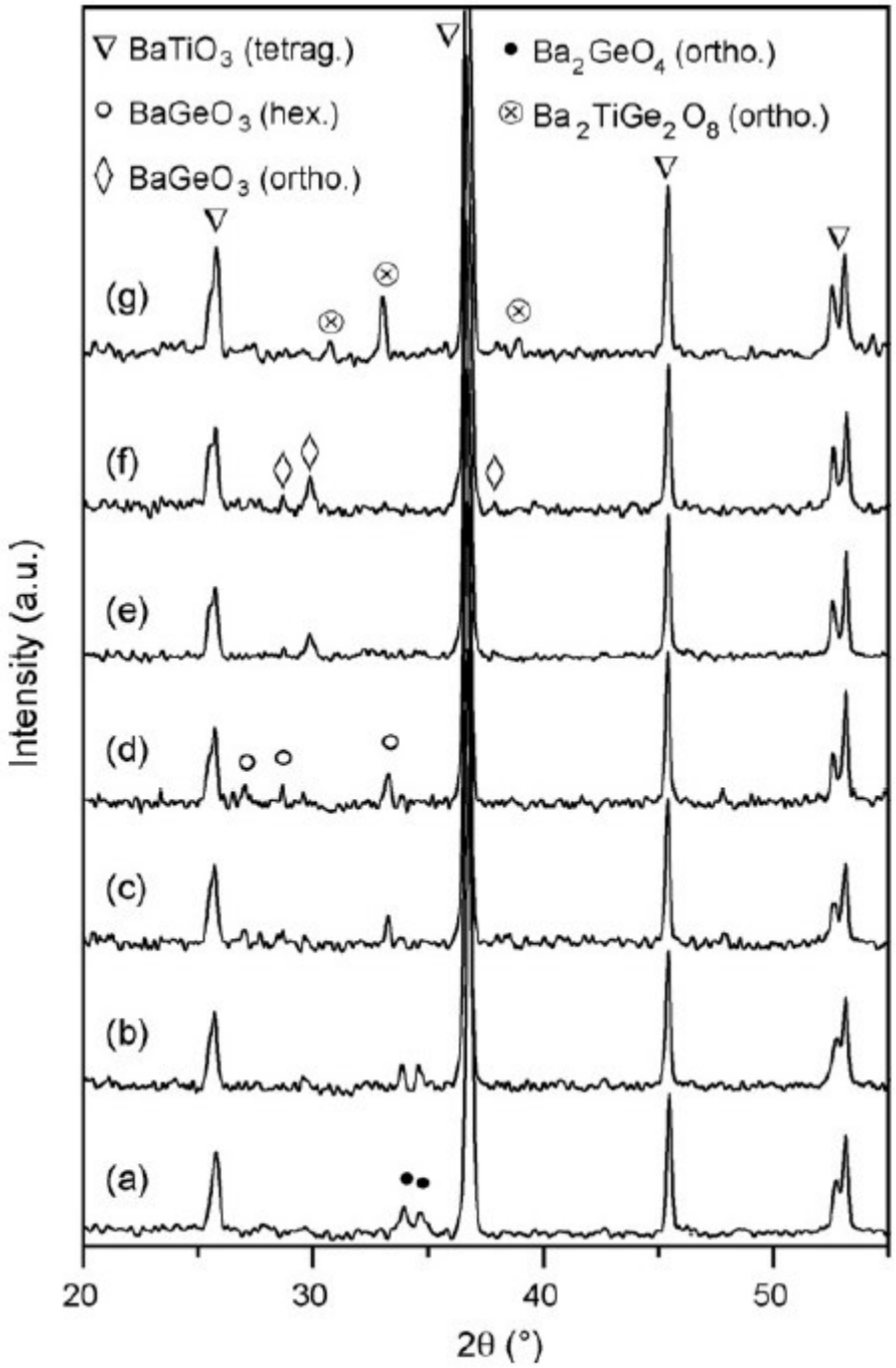


**Fig. 6.** X-ray powder diffraction patterns (recorded at 25 °C) of powder **2** (a) and the resulting ceramic bodies after isothermal sintering (heating rate 10 K min$^{-1}$), (b) 1000 °C, 1 h; (c) 1100 °C, 1 h; (d) 1150 °C, 1 h; (e) 1250 °C, 1 h; (f) 1350 °C, 1 h; (g) 1350 °C, 5 h.